Journal of Sound and Vibration 331 (2012) 4704–4712

Contents lists available at SciVerse ScienceDirect

Journal of Sound and Vibration

journal homepage: www.elsevier.com/locate/jsvi

Micro/macro-slip damping in beams with frictional contact interface

K. Asadi, H. Ahmadian*, H. Jalali

Center of Excellence in Experimental Solid Mechanics and Dynamics, School of Mechanical Engineering, Iran University of Science and Technology, Narmak, Tehran 16844, Iran

ARTICLE INFO

Article history:
Received 19 September 2011
Received in revised form
9 May 2012
Accepted 15 May 2012
Handling Editor: I. Lopez Arteaga
Available online 22 June 2012

ABSTRACT

Friction in contact interfaces of assembled structures is the prime source of nonlinearity and energy dissipation. Determination of the dissipated energy in an assembled structure requires accurate modeling of joint interfaces in stick, micro-slip and macro-slip states. The present paper proposes an analytical model to evaluate frictional energy loss in surface-to-surface contacts. The goal is to develop a continuous contact model capable of predicting the dynamics of friction interface and dissipation energy due to partial slips. To achieve this goal, the governing equations of a frictional contact interface are derived for two distinct contact states of stick and partial slip. A solution procedure to determine stick–slip transition under single-harmonic excitations is derived. The analytical model is verified using experimental vibration test responses performed on a free-frictionally supported beam under lateral loading. The theoretical and experimental responses are compared and the results show good agreements between the two sets of responses.

1. Introduction

There have been extensive investigations on the friction damping effect in the dynamics of build-up structures in the past [1–4]. Friction is the tangential reaction force generated in the interface of the two contacting surfaces while an external force is applied on the assembly. Dry friction is the primary source of nonlinear behavior in structural contact interfaces. It acts as a mechanism to dissipate energy due to relative tangential displacements in the interfaces and may become responsible for 90 percent of the total structure damping [5]. The prediction of energy dissipation due to micro-slip or partial-slip is still an important issue in the structural designs and the subject of many studies. The term "micro-slip" is used where in a small fraction of the entire contact interface the generated shear force reaches a threshold that the contact pressure is insufficient to prevent slip. In the analysis of the structures embedding friction interfaces, it is of interest to propose physical-based accurate micro-slip model to determine the frictional energy loss. Two general types of models are widely used in this regard namely, the lumped parameter models and continuum approaches [6]. The lumped parameter models are in fact different configurations of the bilinear macro-slip element introduced by Iwan [7] and are further developed during the recent years [8–10]. The latter models utilize continuum approaches in which the regions of stick and slip in the contact interface are captured by applying a quasi-static load condition. Rice and Ruina [11] have developed a general rate and state dependent friction law which was related to time-varying contact conditions and relative velocity of the sliding points. This law is applied particularly in steady-sliding stability problems by defining critical stiffness of system. Oden and Martins [12] used a continuum mechanics-motivated approach and derived power

* Corresponding author. Tel.: +98 21 77240198; fax: +98 21 77240488.
E-mail address: ahmadian@iust.ac.ir (H. Ahmadian).

0022-460X/$ - see front matter © 2012 Elsevier Ltd. All rights reserved.
http://dx.doi.org/10.1016/j.jsv.2012.05.026

law expressions for normal and tangential stresses in the contact interface. They used the hyperbolic arctangent function to approximate the friction force smoothing at relative zero velocity so that no sticking state is observed in their model. Menq et al. [13] proposed a partial slip model in which the friction damper is modeled as an elastic rod in contact with an elasto-plastic shear layer under static axial load. The structural response was investigated in full ranges of interface conditions including stick, partial slip and macro-slip. Csaba [14] proposed a micro-slip friction model with a parabolic normal contact load distribution assuming the shear layer has no elastic deformation in stick state and defined slip length based on the model developed in [13]. A single blade with a grounded linear friction damper was analyzed using this model in the frequency domain. The predicted responses when only macro-slip was included in the model were much higher compared to when both micro- and macro-slips were accounted in the model. Cigeroglu et al. [15] further developed the one-dimensional micro-slip model of Menq et al. [13] by including the inertia of the system, and assuming a non-uniform normal contact load distribution. The structure is analyzed for uniform, convex and concave contact normal load distributions and the results are compared with a point contact model.

The present paper extends the rod model with axial motion on frictional support of Refs. [13–15] to a beam model in lateral motion with partial slip on a similar support. The paper proposes a new continuous micro-slip model for a bolted beam in bending which is capable of evaluating the dissipated energy in contact interface via stick–slip transition criteria. For this purpose the contact interface is regarded as a virtual elasto-plastic shear layer between the interface surfaces which takes different states of stiction, partial or micro-slip and macro-slip in the loading cycles according to the shear and normal forces acting in the interface. The systems of governing equations of frictionally supported beam are derived for distinct states of stiction, micro-slip and macro-slip in shear layer by extended Hamilton's principle. Solving the equations of motion analytically for these cases, the structure shows a linear behavior in stiction and nonlinear behavior when micro-slip initiates in the contact interface. The slip initiation and its propagation in the interface are determined using a constraint indicating the transition of shear force from stick to slip state. An experiment is conducted on a test structure and the performance of proposed model is investigated by comparing the predicted and measured hysteresis loops in different excitation harmonics.

2. Governing equations of a beam on frictional support

The governing equations for a frictionally supported beam in bending, as shown in Fig. 1, are derived in this section. The displacement field of the Euler beam is assumed in the form of

$$U(x,z) = u(x) + zw'(x),$$
$$W(x,z) = w(x), \tag{1}$$

in which x and z are Cartesian coordinates and the origin of the coordinate system is on the neutral axis. The total axial displacement of the beam $U(x,z)$ consists of two parts, one caused by displacement of the neutral axis of the beam $u(x)$ and the other by rotation of the beam, i.e. $w'(x)$. The lateral displacement is denoted by $w(x)$. The components of strain and stress fields can be found as

$$\begin{aligned} &\varepsilon_{xx} = u' + zw'', \quad \varepsilon_{xz} = 0, \quad \varepsilon_{zz} = 0, \\ &\sigma_{xx} = E\varepsilon_{xx}, \qquad \sigma_{xz} = 0, \quad \sigma_{zz} = 0. \end{aligned} \tag{2}$$

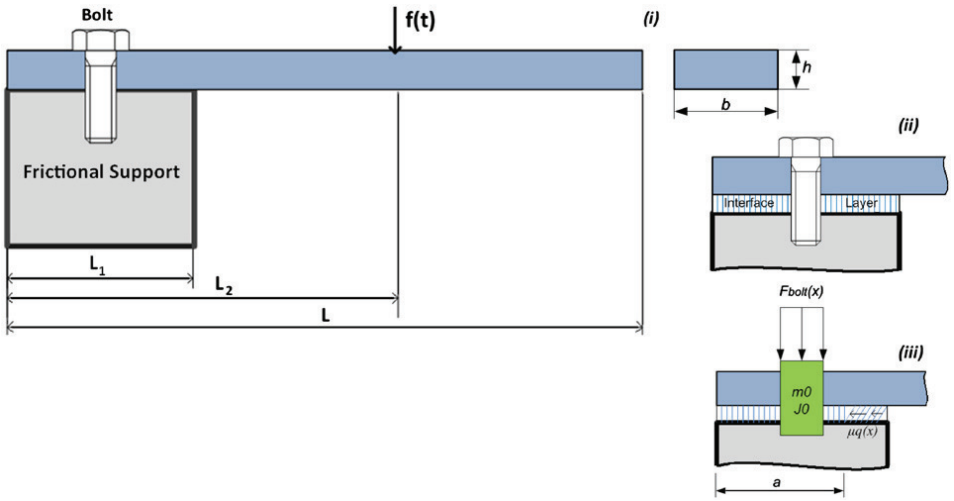

Fig. 1. Free-frictionally supported beam: (i) general view, (ii) the contact interface in stick, and (iii) micro-slip state.

The followings sought derivation of the equations of the motion by means of the extended Hamilton's principle. The extended Hamilton's principle can be expressed in the form

$$\int_{t_1}^{t_2} (\Delta K - \Delta P + \Delta W_{nc})\, \mathrm{d}t = 0 \tag{3}$$

The notations δ and Δ denote "Dirac delta function" and "variation symbol" respectively. The kinetic energy of the structure is expressed as

$$K = \frac{1}{2}\int_V \rho(\dot{U}^2 + \dot{w}^2)\, \mathrm{d}V + \frac{1}{2} m_0 \left(\dot{u}\left(\frac{L_1}{2}\right)^2 + \dot{w}\left(\frac{L_1}{2}\right)^2 \right), \tag{4}$$

where m_0 is the effective mass of the bolt that is located at $x = L_1/2$ and ρ is the beam mass density. The strain energy of the structure is given by

$$P = \frac{1}{2}\int_V \sum_{i,j=1}^{3} \sigma_{ij}\varepsilon_{ij}\, \mathrm{d}V + \frac{1}{2}\int_0^{L_1} k_n w^2(x)\, \mathrm{d}x + \frac{1}{2} k_0 u \left(\frac{L_1}{2}\right)^2, \tag{5}$$

where k_n is the normal stiffness of the support and k_0 is the tangential stiffness at $x = L_1/2$ due to the bolt lateral flexibility.

The work done by tangential contact force is expressed by

$$W_{nc} = \int_0^{L_1} f_h U\, \mathrm{d}x, \tag{6}$$

in which f_h is the shear force acting on the beam. Substituting Eqs. (1) and (2) into Eqs. (4)–(6) and introducing the results into the extended Hamilton's principle of Eq. (3) one obtains

$$\begin{aligned} &\left(\rho A + m_0 \delta\left(x - \tfrac{L_1}{2}\right)\right)\ddot{w} + EIw'''' - \left(\rho I + J_0 \delta\left(x - \tfrac{L_1}{2}\right)\right)\ddot{w}'' + k_n w + \tfrac{h}{2} f_h(x,t) = 0, \\ &\left(\rho A + m_0 \delta\left(x - \frac{L_1}{2}\right)\right)\ddot{u} - EAu'' + k_0 \delta\left(x - \frac{L_1}{2}\right)u + f_h(x,t) = 0, \end{aligned} \tag{7}$$

where A, I, h and b are respectively cross-sectional area, cross-sectional moment of inertia, height and width of the beam and J_0 is the bolt mass moment of inertia. E is Young's modulus. Superscripts $()'$ and $()^{\bullet}$ denote differentiation with respect to x and t, respectively.

Eq. (7) can be further simplified when f_h is functionally known. In order to define the contact force f_h, three different conditions are considered describing the state of the contact interface, i.e. the elastic stick state, micro-slip and the macro-slip conditions.

In stiction the shear layer deforms elastically and none of the contacting bristles yields, i.e. the tangential springs behave linearly. The deformation of the shear layer is proportional to tangential contact force and can be defined using tangential shear stiffness k_t as

$$f_h = k_t U(H(x) - H(x - L_1)), \tag{8}$$

where $H(x)$ is Heaviside function.

Once the shear force at the entire contact interface reaches its slip limit, all the bristles yield and the contact shear force is obtained by using Coulomb friction law as

$$f_h = \mu q_{\mathrm{eff}}(x)(H(x) - H(x - L_1)), \tag{9}$$

where q_{eff} is the effective normal force in the contact interface.

The interface shear force in micro-slip state can be defined using a combination of stiction and macro-slip shear forces in support. In this case a part of support, i.e. $0 < x < a$, is in stiction and the remaining part is in macro-slip, and the support shear force is defined as

$$f_h = k_t U(H(x) - H(x - a)) + \mathrm{sgn}(\dot{U})\mu q_{\mathrm{eff}}(x)(H(x) - H(x - L_1)). \tag{10}$$

Next the dynamic analysis of the beam is considered while the support is in micro-slip.

3. Beam dynamics with micro-slip in support

The structure shown in Fig. 1 is analyzed in the state of stick. The deformation in the interface layer is assumed to be elastic and the structure behaves linearly as presented in section (ii) of this figure. In order to determine stick–slip transition in the contact interface, the elastic contact force between the beam and the support is compared with friction force along the interface. As long as the contact elastic force is less than the frictional force, the contact interface is in the stick regime. The slip happens when the contact elastic force reaches the frictional force at any point of the interface.

In order to determine the beam dynamic behavior, one needs to specify the distribution of normal contact force in the support. The effective static normal contact force is determined in the following section.

3.1. Effective static normal force

The preload of the bolt causes a normal load distribution in the contact interface. The load distribution is a function of beam flexural rigidity and the support normal stiffness. The effect of beam lateral inertial forces on the support section is neglected and the governing equations of beam on support is defined as

$$\begin{aligned} EIw_s'''' + k_n w_s = F_{\text{bolt}}(x), \quad 0 \le x \le L_1, \\ EIw_s'''' = 0, \quad L_1 \le x \le L, \end{aligned} \tag{11}$$

where $F_{\text{bolt}}(x)$ is the preload of the bolt. These equations are subjected to the following boundary and compatibility conditions:

$$w''(0) = w'''(0) = w''(L) = w'''(L) = 0, \tag{12a}$$

$$w_s(L_1^-) = w_s(L_1^+), \quad w_s'(L_1^-) = w_s'(L_1^+), \quad w_s''(L_1^-) = w_s''(L_1^+), \quad w_s'''(L_1^-) = w_s'''(L_1^+). \tag{12b}$$

In Eq. (12a) the boundary conditions are presented; the bending moments and shear forces at two ends of the beam are zero. Eq. (12b) shows the compatibility requirements at $x=L_1$ where the lateral deflections, slopes, bending moments and shear forces for the two beam sections are equal. Solving Eq. (11) leads to the deformed shape of beam on the support and the normal contact force is obtained as a result

$$q_{\text{eff}}(x) = k_n w_s(x). \tag{13}$$

The obtained normal contact force is used to determine the support shear forces.

3.2. Determination of the contact shear forces

The equations of motion of the structure when the contact interface is in stick regime can be rewritten by dividing them into two parts. The first part corresponds to the supported part, i.e. $0 \le x \le L_1$, and the second corresponds to the overhanged portion, i.e. $L_1 \le x \le L$,

$$\begin{aligned} &EIw'''' + \left(\rho I\omega^2 - k_t\tfrac{h^2}{4} + J_0\omega^2\delta\left(x-\tfrac{L_1}{2}\right)\right)w'' + \left(k_n - \rho A\omega^2 - m_0\omega^2\delta\left(x-\tfrac{L_1}{2}\right)\right)w + k_t\tfrac{h}{2}u' = 0, && 0 \le x \le L_1, \\ &EAu'' + \left(\rho A\omega^2 + m_0\omega^2\delta\left(x-\tfrac{L_1}{2}\right) - k_t + k_0\delta\left(x-\tfrac{L_1}{2}\right)\right)u + k_t\tfrac{h}{2}w' = 0, && 0 \le x \le L_1, \\ &EIw'''' + \rho I\omega^2 w'' - \rho A\omega^2 w = f\delta(x-L_2), && L_1 \le x \le L, \\ &EAu'' + \rho A\omega^2 u = 0, && L_1 \le x \le L. \end{aligned} \tag{14}$$

The boundary conditions and compatibility requirements of these two parts are defined as

$$w''(0,\theta) = w'''(0,\theta) = w''(L,\theta) = w'''(L,\theta) = 0, \text{ and } u'(0,\theta) = u'(L,\theta) = 0, \tag{15a}$$

$$\begin{aligned} &w(L_1^-,\theta) = w(L_1^+,\theta), \quad w'(L_1^-,\theta) = w'(L_1^+,\theta), \quad w''(L_1^-,\theta) = w''(L_1^+,\theta), \quad w'''(L_1^-,\theta) = w'''(L_1^+,\theta), \\ &u(L_1^-,\theta) = u(L_1^+,\theta), \quad u'(L_1^-,\theta) = u'(L_1^+,\theta), \quad \text{where } \theta = \omega t. \end{aligned} \tag{15b}$$

The boundary conditions are free–free as represented in Eqs. (15a). The compatibility requirements given in Eqs. (15b) requires the solution of beam segments at $x=L_1$ produces continuous lateral deflections up to the third derivative, and guarantees the continuity of axial deflections up to the first derivatives.

Solving differential equations presented in Eq. (14) together with boundary and compatibility conditions the axial and lateral responses of the beam is obtained. The contact elastic force in the state of stick can be expressed as

$$F_t(x,\theta) = k_t\left(u(x,\theta) - \frac{h}{2}w'(x,\theta)\right). \tag{16}$$

The total normal load depends not only on the preload but also on its dynamic displacement. In other words, the effective normal load is a function of both static and dynamic response of the beam

$$\begin{aligned} F_f(x) = \mu q_{\text{eff}}(x), \\ q_{\text{eff}}(x) = k_n(w_s(x) + w_d(x,\theta)), \end{aligned} \tag{17}$$

where $w_s(x)$ is the beam static deflection due to preload and $w_d(x)$ is dynamic response of the beam. The contact interface transition criteria between slip and sticking states is set by equating the contact shear force and the sliding friction force, i.e.

$$\left|k_t\left(u(x) - \frac{h}{2}w'(x)\right)\right| = \mu(k_n(w_s(x) + w_d(x))). \tag{18}$$

Using this criterion the slip initiation location and hence the minimum force required to initiate slip in the contact interface is determined.

3.3. The structural response in partial slip

As the magnitude of the excitation force increases, the contact force in the shear layer exceeds the allowable value and – depending on the distribution of the contact normal force – a slip region is formed in the interface. The location of the first point undergoing slip depends on the axial and lateral responses of the beam and the distribution of the normal load. In the following it is assumed that the slip initiates from the right side of the contact interface. Therefore, the contact interface is divided into stick and slip regions as is shown in part (iii) of Fig. 1.

The governing equations of the structure is given by

$$\begin{aligned}
&EIw'''' + \left(\rho I\omega^2 - k_t\tfrac{h^2}{4} + J_0\omega^2\delta\left(x-\tfrac{L_1}{2}\right)\right)w'' + \left(k_n - \rho A\omega^2 - m_0\omega^2\delta\left(x-\tfrac{L_1}{2}\right)\right)w + k_t\tfrac{h}{2}u' = 0, && 0\le x\le a,\\
&EAu'' + \left(\rho A\omega^2 + m_0\omega^2\delta\left(x-\tfrac{L_1}{2}\right) - k_t + k_0\delta\left(x-\tfrac{L_1}{2}\right)\right)u + k_t\tfrac{h}{2}w' = 0, && 0\le x\le a,\\
&EIw'''' + \rho I\omega^2 w'' + (k_n - \rho A\omega^2)w - \tfrac{\mu h}{2}k_n(w_s' + w') = 0, && a\le x\le L_1,\\
&EAu'' + \rho A\omega^2 - \mu k_n(w_s + w) = 0, && a\le x\le L_1,\\
&EIw'''' + \rho I\omega^2 w'' - \rho A\omega^2 w = f\delta(x-L_2), && L_1\le x\le L,\\
&EAu'' + \rho A\omega^2 u = 0, && L_1\le x\le L.
\end{aligned} \tag{19}$$

Eqs. (19) are subjected to the following boundary conditions and compatibility equations:

$$w''(0,\theta) = w'''(0,\theta) = w''(L,\theta) = w'''(L,\theta) = 0, \text{ and } u'(0,\theta) = u'(L,\theta) = 0, \tag{20a}$$

$$\begin{aligned}
&w(a^-,\theta) = w(a^+,\theta), \quad w'(a^-,\theta) = w'(L_1^+,\theta), \quad w''(a^-,\theta) = w''(a^+,\theta), \quad w'''(a^-,\theta) = w'''(a^+,\theta),\\
&w(L_1^-,\theta) = w(L_1^+,\theta), \quad w'(L_1^-,\theta) = w'(L_1^+,\theta), \quad w''(L_1^-,\theta) = w''(L_1^+,\theta), \quad w'''(L_1^-,\theta) = w'''(L_1^+,\theta),\\
&u(a^-,\theta) = u(a^+,\theta), \quad u'(a^-,\theta) = u'(a^+,\theta), \quad (L_1^-,\theta) = u(L_1^+,\theta), \quad u'(L_1^-,\theta) = u'(L_1^+,\theta).
\end{aligned} \tag{20b}$$

The boundary conditions are free–free as represented in Eqs. (20a). The compatibility requirements given in Eqs. (20b) requires the solution of beam segments at $x=a$ and L_1 produces continuous lateral deflections up to the third derivative, and guarantees the continuity of axial deflections up to the first derivatives.

It is assumed that the solution of Eqs. (19) has the following form:

$$\begin{aligned}
w(x,t) &= w_s(x) + w_d(x)\sin(\theta),\\
u(x,t) &= u_s(x) + u_d(x)\sin(\theta).
\end{aligned} \tag{21}$$

In Eq. (21) '*s*' and '*d*' refer to static and dynamic responses of the beam, respectively. In compatibility equations of (20b), the length '*a*' is an unknown parameter obtained using an extra constraint implying that the frictional forces at $x=a$ calculated from Eqs. (19)–(21) on the stick side and the slipping side is equal. This constraint is defined as

$$\left|k_t(u(a) - \frac{h}{2}w'(a))\right| = \mu k_n w(a). \tag{22}$$

Solving governing equations together with boundary and compatibility conditions and using the constraint (22), one establishes the backbone curve by incrementally increasing the magnitude of the excitation force. It is worth noting that increasing the amplitude of the harmonic force leads to a multi-region interface. To obtain a solution in such a case, the governing equations as well as the solution procedure should be generalized in a similar fashion that mentioned for a two-region contact interface. The force–displacement backbone curves for linear and nonlinear dynamic behavior of the beam structure are determined and using the Masing rule theoretical hysteresis loops are generated. A typical static load–displacement hysteresis loop obtained by employing the mentioned procedure is illustrated in Fig. 2.

4. Experimental case study

The experimental set-up consists of a single steel beam bolted to a frictional support at one end as shown in Fig. 3.

The beam dimensions are $L=300$ mm (length), $b=30$ mm (width) and $h=3$ mm (thickness). The frictionally supported beam section has a length of $L_1=50$ mm which bolted to the frictional support by means of a M18 bolt. The bolt has mass of 52 g. The structure was excited by a concentrated external force applied by an electromagnetic mini-shaker through a stinger. The excitation location was $x=130$ mm away from the frictional end and the response of the beam was measured at the same point. The bolt was fastened with a torque of 20.4 N m and it was ensured the preload remained constant during the experiment.

Initially the structure was excited with a low-level pseudo-random force within frequency range of 0–400 Hz and the first two natural frequencies of the linear structure were measured. Fig. 4 shows the corresponding FRF of the linear structure indicating two bending modes at the frequencies of 35.40 Hz and 220.80 Hz.

Next the structure was excited using single harmonic forces at different excitation frequencies and the structural responses in acceleration form were measured. The response contains the same harmonic as the excitation force and its multiples due to nonlinear effects in the structure. This makes analytical integration possible to obtain the displacements from measured accelerations. Considering the excitation frequency as ω, a Fourier series of the following form was fitted

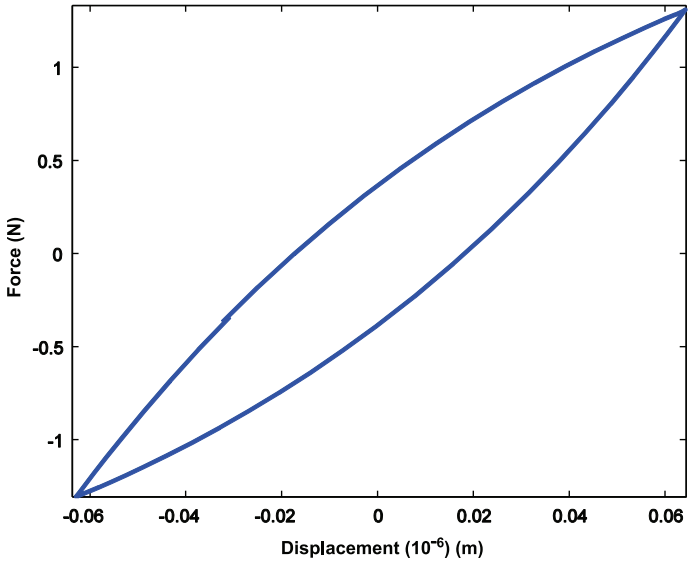

Fig. 2. A typical static loading hysteresis loop.

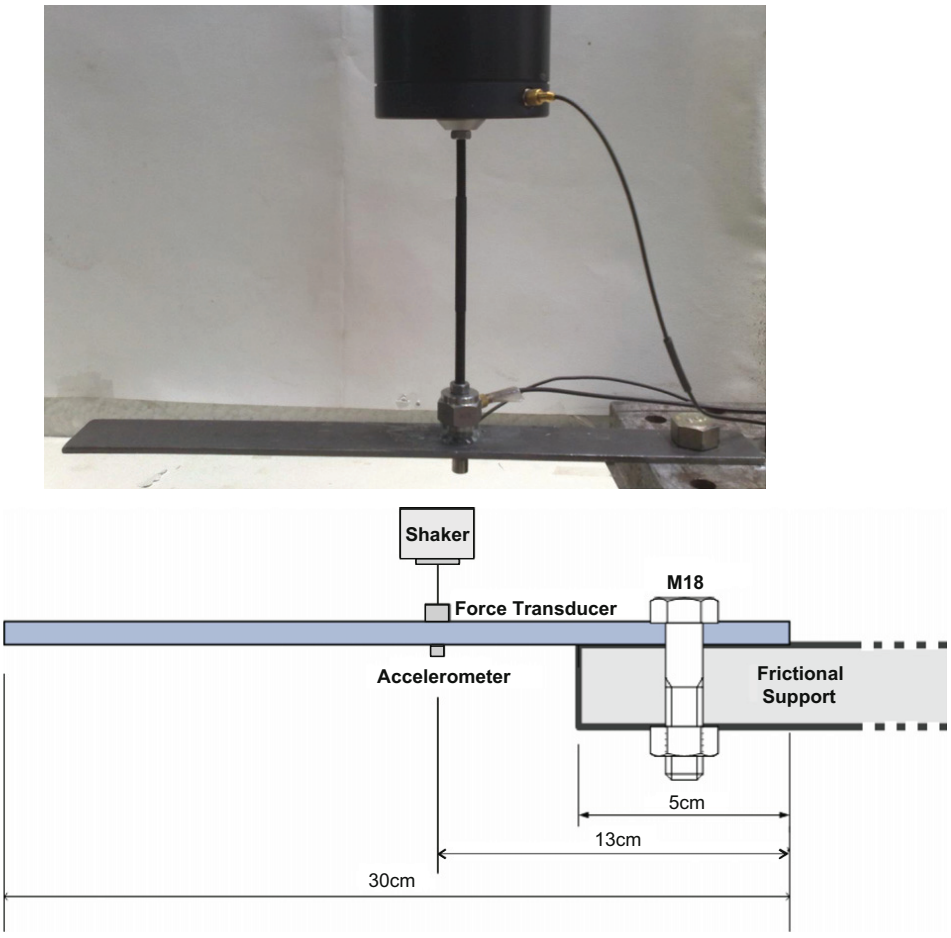

Fig. 3. The test set-up.

to every measured acceleration signal:

$$\ddot{w}(t) = \sum_{m=1}^{M} (A_m \sin(m\omega t) + B_m \cos(m\omega t)), \tag{23}$$

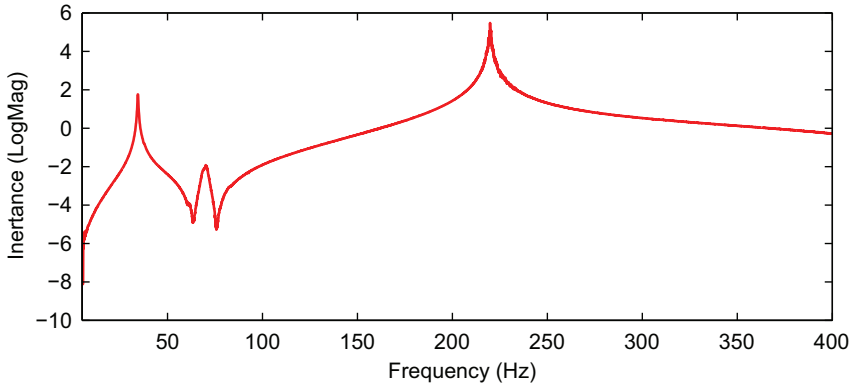

Fig. 4. Frequency responses function of the linear structure.

where the coefficients A_m and B_m are obtained from data fitting. The displacement $w(t)$ is obtained by integrating the acceleration twice as

$$w(t) = -\sum_{m=1}^{M}\left(\frac{A_m}{(m\omega)^2}\sin(m\omega t) + \frac{B_m}{(m\omega)^2}\cos(m\omega t)\right), \tag{24}$$

The hysteresis loops and resultant dissipated energy in the frictional support are obtained using the measured force signals and the corresponding calculated displacement responses.

5. Validating the model predictions

Parameters of the analytical model introduced in Section 3 are known except for the normal and tangential stiffness coefficients of the support, i.e. k_n and k_t respectively.

The beam lateral modes are sensitive to the support normal stiffness k_n therefore this parameter is identified using the first two measured modes of the structure. When k_n is set to zero the beam boundary conditions are free–free and as it approaches infinity shank part of the beam poses clamped–free boundary conditions.

A linear eigen-sensitivity identification procedure is employed and k_n is identified by minimizing the difference between measured lateral modes and the corresponding values predicted by the model. The first two bending modes of the identified model are 35.25 Hz and 219.70 Hz which are very close to the measured natural frequencies of 35.40 Hz and 220.80 Hz.

The support tangential stiffness k_t controls the elastic slope of the hysteresis loops. This parameter is tuned such that the analytical model regenerates the elastic slope of the experimental hysteresis loops. The resulting stiffness coefficients for the analytical model are $k_n = 1.7 \times 10^9$ N/m and $k_t = 5.8 \times 10^8$ N/m. The contact parameters are functions of interface roughness, material and normal preload; as long as they are kept constant these parameters can be used to determine the dynamic behavior even if structure is modified.

In order to evaluate the accuracy of the updated analytical model and applicability of the developed methodology in predicting the beam response, the analytical and experimental hysteresis loops are compared in different frequencies around the first resonant frequency. The selected excitation frequencies are shown in Fig. 5.

The theoretical hysteresis loops are obtained from the analytical updated model according to the procedure described in Section 3. The analytical and experimental hysteresis loops as well as the acceleration auto-spectrums at specific frequencies around the first natural frequency are shown in Figs. 6 and 7.

Fig. 6 indicates under single harmonic excitation the structural response contains higher harmonics which are multiples of the excitation harmonic. This indicates nonlinear behavior of the beam which is due to micro-slips developing at the contact interface. The emerging odd numbers of super-harmonics in the frequency content of the responses suggest that a cubic stiffness nonlinear term exists in the dynamics of the bolted structure. Fig. 6a shows micro-slip is present in the contact interface as only the third higher harmonics is excited. Fig. 6(b)–(d) show even and odd higher harmonics are present in the response caused by the micro-slips and micro-slaps. The later effect is not included in the analytical model.

A good agreement between the predictions of the identified nonlinear model and the measured responses are achieved as shown in Fig. 7. The enclosed area of hysteresis loops indicates the system dissipated energy in one motion cycle. The dissipated energy depends on the length of support with partial slip and the distribution of the normal force at the contact interface. The analytical model is capable of predicting the experimental observations with acceptable accuracy.

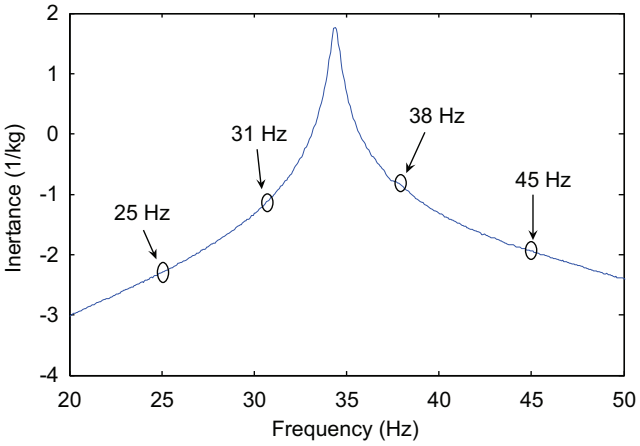

Fig. 5. Selected excitation frequencies around the first mode.

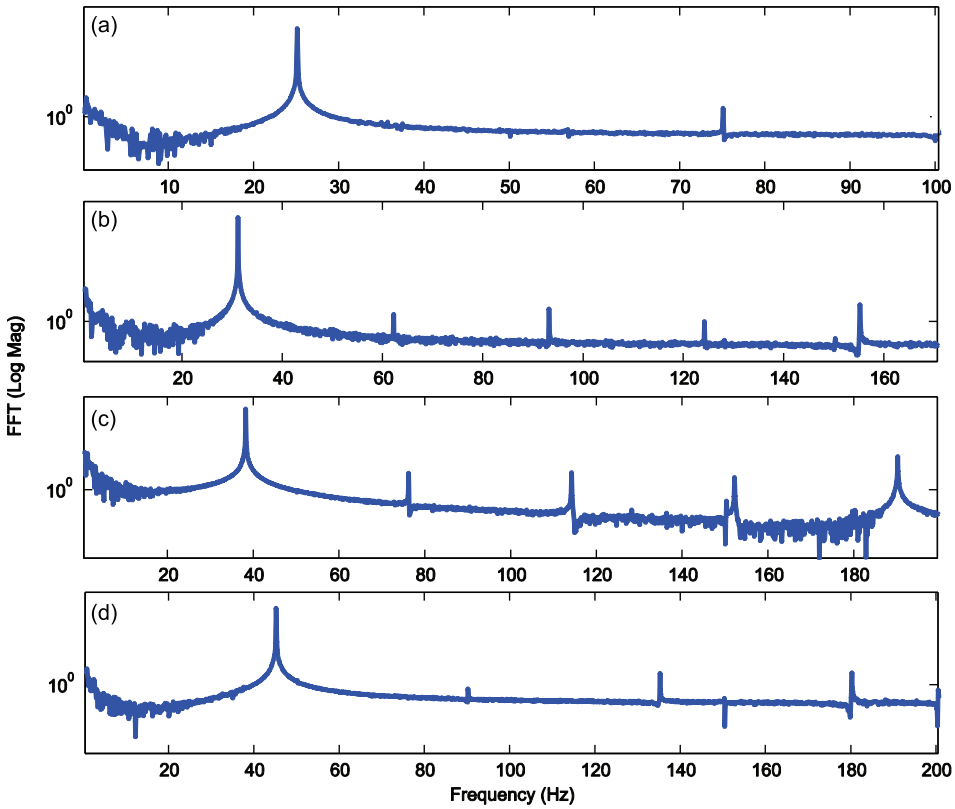

Fig. 6. The auto-spectrums of the measured acceleration responses (m/s^2): 25 Hz (a), 31 Hz (b), 38 Hz (c) and 45 Hz (d).

6. Conclusions

A micro-slip model for evaluation of the energy dissipation in flexural vibration of a bolted beam is presented. An analytical approach is employed to determine the stick–slip transitions of a frictionally supported beam under harmonic excitation. The contact interface parameters are identified using experimentally measured data such that the differences between the model predictions and the experimental observations are minimized. The force–displacement backbone curves for linear and nonlinear dynamic behavior of the beam structure are determined and using the Masing rule theoretical hysteresis loops are generated. The obtained analytical model is capable of accurately regenerating the hysteresis loops and corresponding dissipated energy of the contact interface.

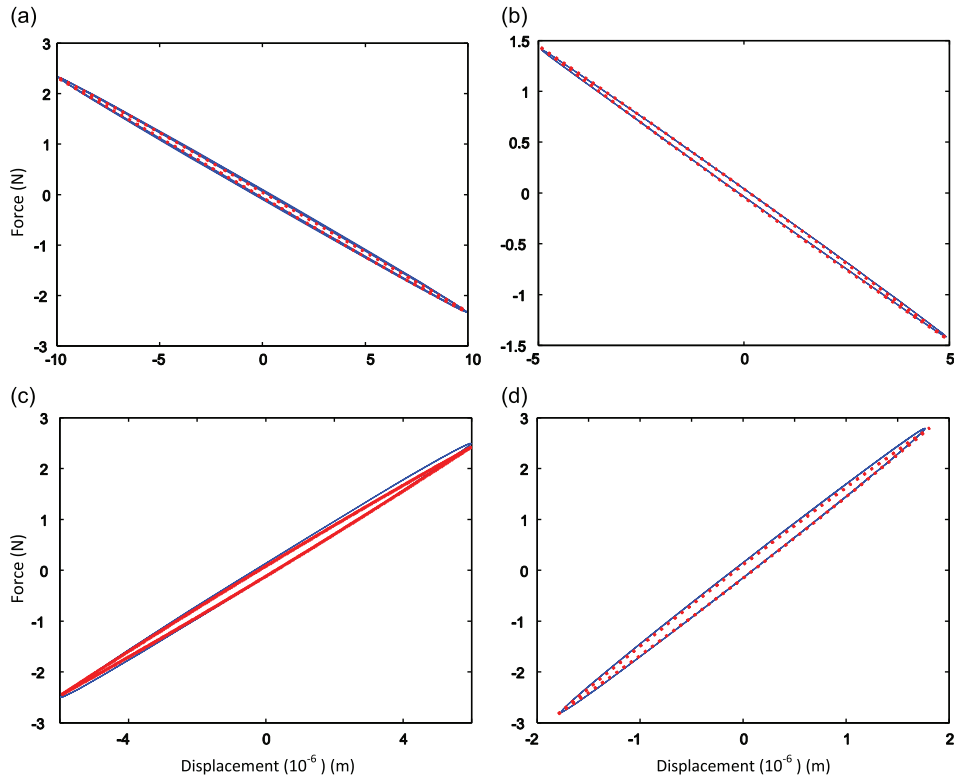

Fig. 7. Analytical (blue lines) and experimental (red dots) hysteresis loops: 25 Hz (a), 31 Hz (b), 38 Hz (c) and 45 Hz (d). (For interpretation of the references to color in this figure legend, the reader is referred to the web version of this article.)

References

[1] L.E. Goodman, J.H. Klumpp, Analysis of slip damping with reference to turbine-blade vibration, *ASME Journal of Applied Mechanics* 23 (1956) 421–429.
[2] T.H.H. Pian, Structural damping of simple built-up beam with riveted joints in bending, *ASME Journal of Applied Mechanics* 24 (1957) 35–38.
[3] A.F. Metherell, S.V. Diller, Instantaneous energy dissipation rate in a lap joint-uniform clamping pressure, *ASME Journal of Applied Mechanics* 35 (1968) 123–128.
[4] E.E. Ungar, The status of engineering knowledge concerning the damping of built-up structures, *Journal of Sound and Vibration* 26 (1973) 141–154.
[5] C.F. Beards, *Structural Vibration: Analysis and Damping*, Arnold, Paris, 1996.
[6] E. Berger, Friction modeling for dynamic system simulation, *Applied Mechanics Reviews* 55 (2002) 535–577.
[7] W. Iwan, A distributed-element model for hysteresis and its steady-state dynamic response, *Journal of Applied Mechanics* 33 (1966) 893–900.
[8] D.D. Quinn, Distributed friction and micro-slip in mechanical joints with varying degrees-of-freedom, *Proceedings of the 2001 ASME Design Engineering Technical Conferences*, Pittsburgh, September 2001.
[9] D.D. Quinn, D.J. Segalman, Using series–series Iwan-type models for understanding joint dynamics, *Journal of Applied Mechanics, Transactions of the ASME* 72 (2005) 778–784.
[10] J.D. Miller, D.D. Quinn, A two-sided interface model for dissipation in structural systems with frictional joints, *Journal of Sound and Vibration* 321 (2009) 201–219.
[11] J.R. Rice, A.L. Ruina, Stability of steady frictional slipping, *Journal of Applied Mechanics* 50 (1983) 343–349.
[12] J.T. Oden, J.A.C. Martins, Models and computational methods for dynamic friction phenomena, *Computer Methods in Applied Mechanics and Engineering* 52 (1985) 527–634.
[13] C.H. Menq, J. Bielak, J.H. Griffin, The influence of microslip on vibratory response—part I: a new microslip model, *Journal of Sound and Vibration* 107 (1986) 279–293.
[14] G. Csaba, Forced response analysis in time and frequency domains of a tuned bladed disk with friction dampers, *Journal of Sound and Vibration* 214 (1998) 395–412.
[15] E. Cigeroglu, W. Lu, C.H. Menq, One dimensional dynamic microslip friction model, *Journal of Sound and Vibration* 292 (2006) 881–898.